Neurobiology of Disease

Roles of Volume-Sensitive Chloride Channel in Excitotoxic Neuronal Injury

Hana Inoue and Yasunobu Okada
Department of Cell Physiology, National Institute for Physiological Sciences, Okazaki 444-8585, Japan

Excitotoxicity is associated with stroke, brain trauma, and a number of neurodegenerative disorders. In the brain, during excitotoxic insults, neurons undergo rapid swelling in both the soma and dendrites. Focal swellings along the dendrites called varicosities are considered to be a hallmark of acute excitotoxic neuronal injury. However, it is not clear what pathway is involved in the neuronal anion flux that leads to the formation and resolution of excitotoxic varicosities. Here, we assessed the roles of the volume-sensitive outwardly rectifying (VSOR) Cl^- channel in excitotoxic responses in mouse cortical neurons. Whole-cell patch-clamp recordings revealed that the VSOR Cl^- channel in cultured neurons was activated by NMDA exposure. Moreover, robust expression of this channel on varicosities was confirmed by on-cell and nystatin-perforated vesicle patch techniques. VSOR channel blockers, but not blockers of $GABA_A$ receptors and Cl^- transporters, abolished not only varicosity resolution after sublethal excitotoxic stimulation but also necrotic death after sustained varicosity formation induced by prolonged NMDA exposure in cortical neurons. The present slice-patch experiments demonstrated, for the first time, expression of the VSOR Cl^- channels in somatosensory pyramidal neurons. NMDA-induced necrotic neuronal death in slice preparations was largely suppressed by a blocker of the VSOR Cl^- channel but not of the $GABA_A$ receptor. These results indicate that VSOR Cl^- channels exert dual, reciprocal actions on neuronal excitotoxicity by serving as major anionic pathways both for varicosity recovery after washout of an excitotoxic stimulant and for persistent varicosity formation under prolonged excitotoxic insults leading to necrosis in cortical neurons.

Key words: **anion channel; cortical neuron; excitotoxicity; necrosis; varicosity; volume regulation**

Introduction

Excitotoxicity, a term coined by Olney (1969), is defined as the excitatory amino acid-mediated degeneration of neurons and is a common pathway in a number of acute neurologic diseases and chronic neurodegenerative disorders. The formation of neuronal dendritic varicosities associated with somatic swelling is an early consequence of excitotoxicity. Varicosities have also been observed as a hallmark of injury in neurons under various pathological conditions *in vivo*, such as ischemia (Hsu and Buzsáki, 1993; Hori and Carpenter, 1994; Matesic and Lin, 1994), epilepsy (Westrum et al., 1964; Scheibel et al., 1974; Reid et al., 1979; Isokawa and Levesque, 1991; Multani et al., 1994), brain tumor (Goel et al., 2003), Huntington's disease (Sotrel et al., 1993), and scrapie infection (Hogan et al., 1987).

Several previous studies reported that the formation of varicosities is reversible, if the excitotoxic stimulus is sublethal, both *in vitro* (Park et al., 1996; Faddis et al., 1997; Hasbani et al., 1998, 2001; Ikegaya et al., 2001) and *in vivo* (Zhang et al., 2005). Although Faddis et al. (1997) reported that calpain is involved in the dendritic remodeling, it is still unclear how this recovery from varicosities is accomplished after sublethal excitotoxicity. Recently, we have observed expression of the volume-sensitive outwardly rectifying (VSOR) Cl^- channel, which is activated and involved in volume regulation in swollen cortical neurons (Inoue et al., 2005). However, it remains unknown whether the VSOR Cl^- channel is activated by excitotoxic swelling and whether it is involved in volume regulation after excitotoxic varicosity formation. Thus, the first purpose of the present study was to address these questions.

The ionic mechanism of excitotoxicity may consist of both a component that mediates NaCl entry and a component that mediates Ca^{2+} inflow (Choi, 1987; Goldberg and Choi, 1993; Dessi et al., 1994). Cl^- entry has been shown to be a key mediator of the acute excitotoxicity marked by somatic and dendritic swelling (Rothman, 1985; Olney et al., 1986; Choi, 1987; Nicklas et al., 1987; Dessi et al., 1994; Hasbani et al., 1998). The Cl^- influx is mediated by multiple pathways. $GABA_A$ receptor-coupled anion channels appear to serve as one of the Cl^- influx pathways in excitotoxic neurons, because $GABA_A$ receptor blockers partially blocked excitotoxic injury (Hasbani et al., 1998; Chen et al., 1999; Babot et al., 2005). Also, an involvement of some other anion channel in the excitotoxic Cl^- influx was suggested (Hasbani et al., 1998; Inglefield and Schwartz-Bloom, 1998; Van Damme et al., 2003; Babot et al., 2005). Thus, the second purpose of this study was to identify the anion channel, which serves as a GABA-independent Cl^- influx pathway during excitotoxicity in cortical neurons.

Because necrotic cell death is known to be associated with

Received Oct. 19, 2005; revised Dec. 19, 2006; accepted Dec. 24, 2006.
We thank R. Z. Sabirov for his helpful discussion throughout this study and E. L. Lee for reviewing this manuscript. M. Ohara and T. Okayasu are gratefully acknowledged for technical and secretarial assistance.
Correspondence should be addressed to Yasunobu Okada at the above address. E-mail: okada@nips.ac.jp.
DOI:10.1523/JNEUROSCI.4694-06.2007
 0270-6474/07/271445-11$15.00/0

persistent cell swelling, called necrotic volume increase (NVI) (Barros et al., 2001; Okada et al., 2001, 2004), there is a possibility that under excitotoxic conditions, neuronal cell death is the consequence of dendritic and somatic swelling caused by persistent Cl^- influx via this GABA-independent pathway. Thus, the third purpose of this study was to test this possibility.

Materials and Methods

Chemicals. All the reagents, except for 4-aminopyridine (4-AP; Wako, Osaka, Japan), nystatin (Wako), tetrodotoxin (TTX; Wako), NMDA (Tocris, Ballwin, MO), (5*S*,10*R*)-(+)-5-methyl-10,11-dihydro-5*H*-dibenzo[a,d]-cyclohepten-5,10-imine maleate (MK801; Tocris), 5-nitro-2-(3-phenylpropylamino)benzoic acid (NPPB; Tocris), EGTA (Dojindo, Kumamoto, Japan), and quinine (Nacalai Tesque, Kyoto, Japan), were obtained from Sigma (St. Louis, MO). NPPB, phloretin, bicuculline, furosemide, bumetanide, indanyloxyacetic acid 94 (IAA-94), and cyclothazide were dissolved in dimethyl sulfoxide (DMSO) to make stock solution and diluted 1000 times in the corresponding bath solution. Picrotoxin was dissolved in ethanol to make stock solution and diluted 500 times for use. (2*R*)-2-amino-5-phosphonopentanoic acid (APV), MK801, NMDA, glycine, and AMPA were dissolved in distilled water to make stock solution and diluted 1000 times for use. No significant effects were observed when vehicle was applied alone.

Cell culture. Neuronal cell cultures derived from mouse embryonic cerebral cortices were prepared, as described previously (Inoue et al., 2005). Briefly, on day 16 of pregnancy, gravid C57BL/6Cr Slc mice were anesthetized with halothane, and the uteri were removed. The cerebral cortex was removed from fetuses and digested using papain (10 U/ml; Worthington Biochemical, Lakewood, NJ). Dissociated cells were plated (0.2×10^6 cells/cm^2) on 0.2% polyethyleneimine-coated glass coverslips. Cells were grown in DMEM supplemented with 10% heat-inactivated fetal bovine serum (HyClone Laboratories, Logan, UT), 0.5 mM glutamine, MITO+ serum extender (Becton Dickinson Labware, Bedford, MA), 100 U/ml penicillin (Meiji, Tokyo, Japan), and 0.1 mg/ml streptomycin (Meiji). To prevent growth of non-neuronal cells, cytosine arabinoside (10 μM) was added to the cultures 24 h after plating. The cultures were maintained in a 5% CO_2 incubator at 37°C and were used after 6–8 d. Our preliminary immunostaining studies showed that, under the present culture conditions, the major cell population comprises glutamatergic neurons reactive to anti-CaMK II antibody, whereas only the minor population comprises GABAergic neurons reactive to anti-GAD antibody (our unpublished observations).

EGFP transfection. Neurons were transfected on day 3 of culture with the plasmid pEGFP-N1 (ClonTech, Palo Alto, CA) using a calcium phosphate method as described previously (Watanabe et al., 1999). In brief, culture medium was replaced with transfection medium, which was culture medium that was serum- and antibiotic-free. The calcium phosphate-plasmid suspension solution (2 μg of plasmid) was added to each culture dish and kept for 1 h in a 5% CO_2 incubator at 37°C. After three washes with transfection medium, the neurons were maintained in culture medium equilibrated with 5% CO_2 at 37°C. The efficiency of transfection was routinely <0.1%. Green fluorescent protein (GFP) fluorescence revealed the neuronal arbor, including axons and dendrites.

Brain slice preparation. Coronal brain slices (300 μm thick) of somatosensory barrel cortex were prepared from young adult (19- to 28-d-old) C57BL/6Cr Slc mice. Mice were deeply anesthetized with halothane and killed by decapitation. The brain was removed rapidly, chilled at 0–4°C in cutting solution containing the following (in mM): 120 choline-Cl, 3 KCl, 1.25 NaH_2PO_4, 28 $NaHCO_3$, 8 $MgCl_2$, and 25 glucose, saturated with carbogen (95% O_2, 5% CO_2), and then sliced using a vibratome (Microslicer ZERO 1; Dosaka, Kyoto, Japan). Slices were incubated at 32°C for 30 min and at room temperature (24–27°C) in carbogen-saturated artificial CSF (ACSF) containing the following (in mM): 125 NaCl, 2.5 KCl, 2 $CaCl_2$, 2 $MgCl_2$, 26 $NaHCO_3$, 1.25 NaH_2PO_4, and 11 glucose.

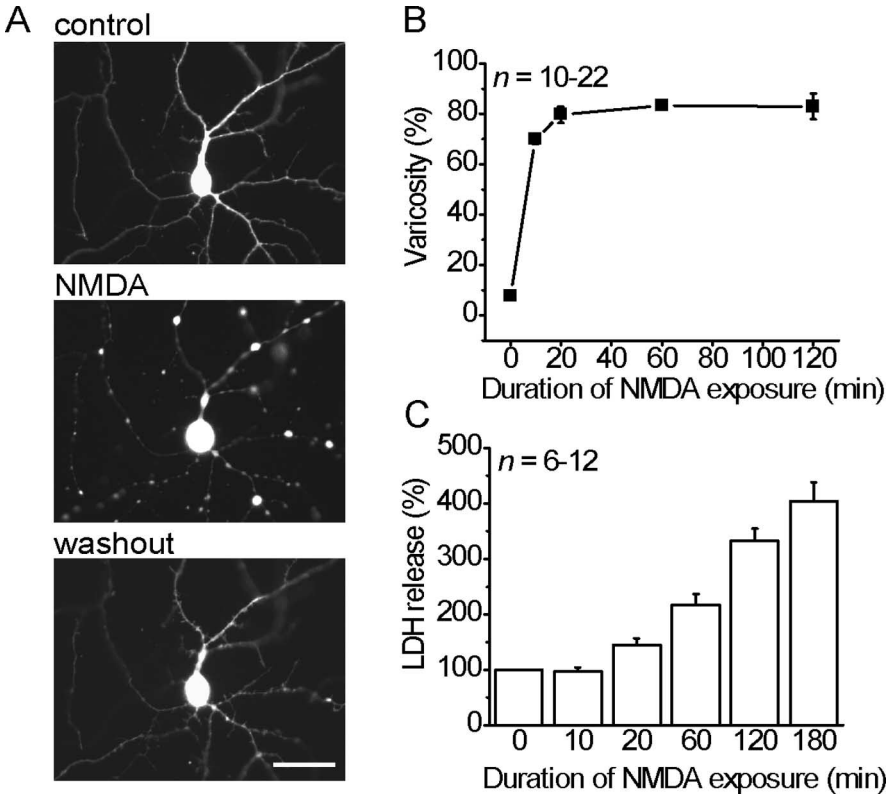

Figure 1. Varicosity formation and necrotic cell death induced by NMDA receptor activation in cultured mouse cortical neurons. ***A***, Images of an EGFP-expressing neuron before (top) and 10 min after (middle) exposure to NMDA as well as 60 min after NMDA removal (bottom). Scale bar, 30 μm. ***B***, Time course of varicosity formation after exposure to NMDA. Cultures were exposed to 30 μM NMDA and fixed at each time point (0, 10, 20, 60, 120 min). The number of EGFP-expressing or DiI-labeled neurons displaying varicosities, as a percentage of the total number of counted neurons, is represented on the *y*-axis. Each symbol represents the mean ± SEM (error bars). ***C***, Time course of NMDA-induced LDH release. Neuronal death was assessed by LDH release 10, 20, 60, 120, and 180 min after exposure to 30 μM NMDA. Each column represents the mean ± SEM (error bars).

Excitotoxicity induction. To induce excitotoxicity in primary cultured cortical neurons, the cultures, in a 5% CO_2 incubator at 37°C, were exposed to 30 μM NMDA and 30 μM glycine for varying time periods in low-Mg^{2+} HEPES/bicarbonate-buffered solution (low-Mg^{2+} HBS) containing the following (in mM): 116 NaCl, 5.4 KCl, 0.5 $MgCl_2$, 2 $CaCl_2$, 1 NaH_2PO_4, 12 HEPES, 25 $NaHCO_3$, and 5.5 glucose, pH 7.4, adjusted with NaOH, 315 mOsm/kg-H_2O adjusted by adding mannitol. Glycine was added to increase the open probability of the NMDA receptor (Johnson and Ascher, 1987). In some experiments, the excitotoxic period was followed by a recovery period. After excitotoxic stimulation, cultures were gently washed three times with PBS, and then incubated in HBS, which consisted of low-Mg^{2+} HBS supplemented with 2 mM $MgCl_2$, for different time periods in a 5% CO_2 incubator at 37°C.

To induce excitotoxicity in brain slices, slices were exposed to 30 μM NMDA in ACSF bubbled with carbogen at room temperature for 1 h.

Assessment of dendritic varicosity formation. Cultures were fixed with 4% paraformaldehyde at the appropriate time points. The presence of dendritic varicosities in EGFP-expressing neurons was determined at 300× under epifluorescence illumination in a blinded manner. Alternatively, fixed cultures were stained with the carbanocyanine membrane

tracer DiI$(C_{18})_3$ to visualize dendritic morphology, using a method, with some modifications, from a previous study (Hasbani et al., 1998). A DiI stock solution of 5 mg/ml was prepared in ethanol and stored at −20°C. The stock was diluted 1000 times in PBS and then cultures were exposed to DiI solution for 2–5 min at room temperature (24–27°C), after which they were washed with PBS. A varicosity was defined as a spherical swelling on a dendrite with diameter >2 μm. Neurons were counted as beaded when they displayed at least one varicosity anywhere along their dendritic arbors. The percentage of neurons displaying varicosities was determined by counting at least 150 cells in each culture well.

Assessment of cell death. In cultured neurons, cell death was assessed by propidium iodide (PI) uptake using an epifluorescence microscope. Cultures were incubated with HBS containing PI (1 μg/ml) and Hoechst 33342 (5 μg/ml) at room temperature for 15 min. Cell mortality was expressed as the ratio of PI-positive cells to total cell number determined by counting cells with chromosomal staining by Hoechst 33342. Cell death in cultures was also assessed by a lactate dehydrogenase (LDH) release assay using the CytoTox-ONE Homogeneous Membrane Integrity Assay (Promega, Madison, WI) according to the manufacturer's instructions.

In brain slices, cell death was assessed by PI staining. PI-positive spots (nuclei) in the somatosensory cortical area (1.3 × 1.8 mm^2) were counted automatically by Image Master 2D Platinum software (GE Healthcare, Buckinghamshire, England).

Caspase-3 activity was measured in primary cultured neurons using a fluorometric assay, as described previously (Maeno et al., 2000). In brief, the difference in fluorescence caused by caspase-3 cleavage of a fluorogenic substrate in the absence and presence of a caspase-3 inhibitor was observed. The fluorogenic substrate for caspase-3, (Ac-DEVD-AMC), which was labeled with the fluorochrome AMC, and the tetrapeptide inhibitor of caspase-3, (Ac-DEVD-CHO) were provided in the CaspACE Assay System (Promega).

Patch-clamp experiments in cultured neurons. All experiments were conducted at room temperature. A salt bridge containing 3 M KCl in 2% agarose was used to connect a reference Ag-AgCl electrode. Liquid junction potentials were calculated using pClamp software (version 8.2; Molecular Devices, Union City, CA) and compensated for when necessary. Currents were recorded using an Axopatch 200A or B amplifier (Molecular Devices) coupled to DigiData 1321A A/D and D/A converters (Molecular Devices). Current signals were filtered at 1 kHz using a four-pole Bessel filter and digitized at 5 or 10 kHz. pClamp 9.0 software was used for the command pulse protocol, data acquisition, and analysis. WinASCD software (provided by Dr. G. Droogmans, Katholieke Universiteit, Leuven, Belgium) was also used for data analysis of single-channel currents.

For whole-cell recordings, patch pipettes were fabricated from borosilicate glass capillaries (outer diameter, 1.4 mm; inner diameter, 1.0 mm; Asahi Rika-Glass Industry, Nagoya, Japan) using a micropipette puller (model P-97; Sutter Instruments, Novato, CA). The electrode had a resistance of 3.5–5 MΩ when filled with pipette solution. The series resistance (<25 MΩ) was compensated by 70% to minimize voltage errors. The time courses of current activation and recovery were monitored by repetitively applying (every 15 s) alternating step pulses (2 s duration) of ±60 mV from a holding potential of −40 mV, which is nearly equal to E_{Cl} (equal to −40.8 mV). During agonist exposure, the membrane potential was held at −40 mV. To observe voltage dependence of the current profile, step pulses were applied from the holding potential to test potentials of −100 to +40 mV in 20 mV increments. To observe inactivation kinetics at strong depolarizing potentials, step pulses up to +120 mV were applied.

The NMDG-Cl bath solution used for monitoring whole-cell Cl^- currents was composed of the following (in mM): 124 *N*-methyl-D-glucamine (NMDG), 124 HCl, 10 NaCl, 4 $MgCl_2$, 0.33 NaH_2PO_4, 0.5 EGTA, 10 HEPES, 2 4-AP, 45 mannitol, and 5.5 glucose, pH 7.4 adjusted with NMDG, 315 mOsm/kg-H_2O. The pipette (intracellular) solution contained the following (in mM): 124 NMDG, 24 HCl, 100 aspartate, 2 $MgCl_2$, 5 Na_2ATP, 0.3 Na_3GTP, 1 EGTA, and 10 HEPES, pH 7.4 adjusted with NMDG, and the osmolality was adjusted to 300 mOsm/kg-H_2O by adding mannitol. When aspartate permeability was examined, intracellular chloride was decreased to 10 mM by replacing with aspartate and the VSOR Cl^- current was elicited by application of hypotonic solution prepared by removing mannitol in the NMDG-Cl bath solution. The bath solution for NMDA exposure experiments contained the following (in mM): 142 NaCl, 0.5 $MgCl_2$, 0.33 NaH_2PO_4, 0.5 EGTA, 10 HEPES, 2

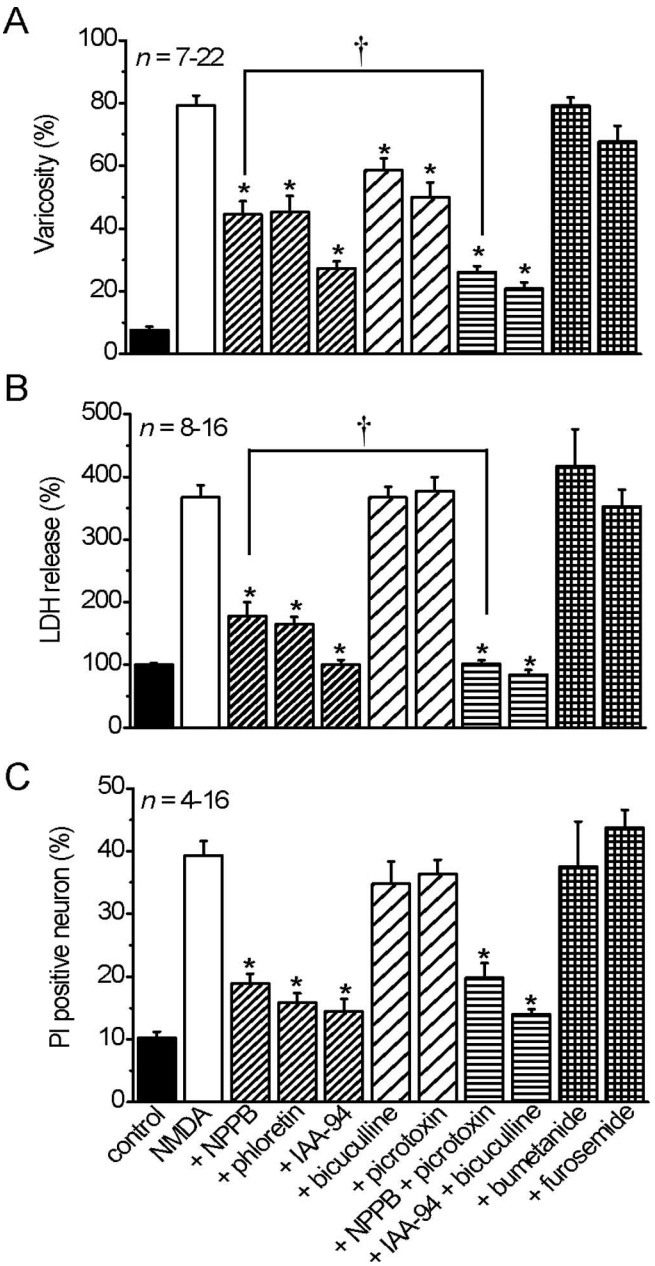

Figure 2. Effects of blockers of Cl^- channels or transporters on varicosity formation and necrotic cell death induced by NMDA exposure in cultured mouse cortical neurons. ***A–C***, Varicosity formation (***A***), LDH release (***B***), and PI uptake (***C***) were assessed 20 min, 3 h, and 3 h, respectively, after application of 30 μM NMDA in the absence and presence of VSOR Cl^- channel blockers (NPPB 40 μM, phloretin 100 μM, IAA-94 1 mM), $GABA_A$ receptor blockers (bicuculline 10 μM, picrotoxin 100 μM), and Cl^- cotransporter blockers (bumetanide 10 μM, furosemide 1 mM). On the varicosity formation (***A***), there was no statistically significant difference between the effect of NPPB or phloretin and that of bicuculline or picrotoxin, whereas the inhibiting effect of IAA-94 was significantly stronger than that of bicuculline or picrotoxin. On the NMDA-induced neuronal cell death (***B***, ***C***), the effect of each of three Cl^- channel blockers was significantly different from that of either $GABA_A$ receptor blocker. $^*p < 0.05$ versus NMDA exposure in the absence of drugs. $^\dagger p < 0.05$ between NMDA exposure in the presence of 40 μM NPPB and that in the combined presence of 40 μM NPPB and 100 μM picrotoxin. Each symbol represents the mean ± SEM (error bars).

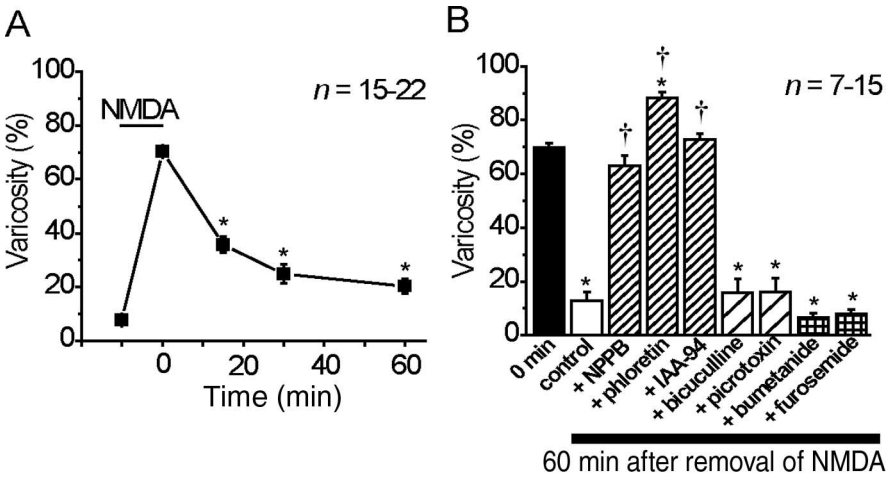

Figure 3. Varicosity resolution after removal of NMDA and its sensitivity to blockers of Cl^- channels or transporters in cultured mouse cortical neurons. ***A***, Time course of recovery from varicosities after termination of sublethal exposure to NMDA (30 μM for 10 min). ***B***, Effects of VSOR Cl^- channel blockers (NPPB 40 μM, phloretin 100 μM, IAA-94 1 mM), $GABA_A$ receptor blockers (bicuculline 10 μM, picrotoxin 100 μM), and Cl^- cotransporter blockers (bumetanide 10 μM, furosemide 1 mM) on recovery from varicosities after removal of NMDA (30 μM for 10 min). $^*p < 0.05$ versus 0 min. $^\dagger p < 0.05$ versus control. Each symbol or column represents the mean ± SEM (error bars).

4-AP, 5.5 glucose, 0.03 NMDA, and 0.03 glycine, pH 7.4 adjusted with NaOH, 315 mOsm/kg-H_2O. For AMPA-exposure experiments the bath solution contained the following (in mM): 142 NaCl, 4 $MgCl_2$, 0.33 NaH_2PO_4, 0.5 EGTA, 10 HEPES, 2 4-AP, 5.5 glucose, 0.001 AMPA, and 0.0025 cyclothiazide, pH 7.4 adjusted with NaOH, 315 mOsm/kg-H_2O. Cyclothiazide was added to inhibit desensitization of the AMPA receptor (Yamada and Tang, 1993). Na^+-free NMDG-Cl bath solution was made by replacing NaCl with NMDG-Cl and eliminating NaH_2PO_4. Hypertonic solution was made by adding 130 mM mannitol to the NMDG-Cl solution. In some experiments, to visualize cell morphology during whole-cell current recordings, 5 μM calcein (Sigma) was added to the pipette solution. Fluorescence images were captured using a CCD camera (ORCA-ER-1394; Hamamatsu Photonics, Hamamatsu, Japan) and recorded using AquaCosmos software (version 2.0; Hamamatsu Photonics).

Single-channel recordings from varicosities were performed in both on-varicosity and perforated-vesicle outside-out configurations. On-cell recordings on dendritic varicosities were performed during excitotoxic stimulation using a pipette solution containing the following (in mM): 124 CsCl, 20 tetraethylammonium (TEA)-Cl, 2 4-AP, 4 $MgCl_2$, 0.5 EGTA, 10 HEPES, and 5.5 glucose, pH 7.4 adjusted with CsOH, 315 mOsm/kg-H_2O. The bath solution was low-Mg^{2+} HBS containing 30 μM NMDA and 30 μM glycine throughout the experiments. Nystatin-perforated-vesicle outside-out recordings were performed as described previously (Levitan and Kramer, 1990) to observe effects of extracellular application of NPPB. The pipette solution contained the following (in mM): 145 KCl, 1 $MgCl_2$, 1 EGTA, and 10 HEPES, pH 7.4 adjusted with KOH, 300 mOsm/kg-H_2O. Nystatin stock solution (60 mg/ml in DMSO) was added to the pipette solution to a final concentration of 0.3 mg/ml. The tip of the patch pipette was filled with nystatin-free pipette solution, and then the remainder of the pipette was back-filled with the nystatin-containing pipette solution. The patch pipette had a resistance of 3–5 MΩ when filled with pipette solution. After the formation of varicosities resulting from exposure to low-Mg^{2+} HBS containing 30 μM NMDA and 30 μM glycine, a gigaohm seal was formed on a varicosity of an EGFP-expressing neuron visualized under fluorescence illumination. When the series resistance decreased to <50 MΩ, the pipette was withdrawn from the cell to form a perforated vesicle. Current recordings were performed in the bath solution, which was identical to the pipette solution used for on-varicosity recordings.

Patch-clamp experiments in brain slices. All experiments were conducted at 37°C. Whole-cell voltage-clamp recordings were made from layer V pyramidal neurons of mouse barrel cortex. The neurons were visually identified by their location and shape using an upright microscope equipped with a 40× water-immersion objective (BX51WI; Olympus Optical, Tokyo, Japan) and infrared differential interface contrast video system (C2741–79; Hamamatsu Photonics). Membrane currents were recorded using a patch-clamp amplifier (EPC-9; HEKA Elektronik, Lambrecht/Pfalz, Germany). Current signals were filtered at 1 kHz using a four-pole Bessel filter and digitized at 10 kHz. Data acquisition and analysis were done using Pulse+PulseFit (HEKA Elektronik) and SigmaPlot (version 7.1; Systat Software, Richmond, CA). Patch pipettes were fabricated and step pulses were applied, as done for whole-cell recordings in cultured neurons. The isotonic bath solution, which was bubbled with carbogen, contained the following (in mM): 80 choline-Cl, 20 TEA-Cl, 2.5 KCl, 1.25 NaH_2PO_4, 2 4-AP, 4 $MgCl_2$, 26 $NaHCO_3$, 11 glucose, 0.0001 TTX, and 55 mannitol (300 mOsm/kg-H_2O). The hypotonic bath solution was made by omitting mannitol (245 mOsm/kg-H_2O). The pipette solution contained the following (in mM): 120 NMDG, 120 gluconate, 4 $MgCl_2$, 5 Na_2ATP, 0.3 Na_3GTP, 1 EGTA, and 10 HEPES, pH 7.4 adjusted with NMDG, 260 mOsm/kg-H_2O. To study anion permeability, extracellular 80 mM choline-Cl was substituted with 160 mM mannitol. To test the effect of intracellular ATP on whole-cell current activation, Na_2ATP was omitted from the pipette solution.

Statistical analysis. Data are given as means ± SEM of observations (n). Comparisons of two experimental groups were made using Student's t *test*, whereas multiple comparisons were made using ANOVA followed by the Bonferroni test. Data were considered to be significant at $p < 0.05$.

Results

Dendritic swelling and necrotic neuronal cell death induced by glutamate receptor stimulation

In cultured mouse cortical neurons, application of the glutamate receptor agonist NMDA (30 μM) for 10 min induced not only somatic swelling but also focal swelling along the dendrites in ~70% of the cortical neurons (Fig. 1*A*,*B*). Consistent with previous reports (Park et al., 1996, Faddis et al., 1997; Hasbani et al., 1998, 2001; Ikegaya et al., 2001), these dendritic beadings or varicosities were resolved spontaneously after washout of NMDA, when its exposure was brief (Fig. 1*A*). As the duration of NMDA exposure increased, the population of neurons with varicosities increased (Fig. 1*B*), and the rate of cell death monitored by LDH release also increased (Fig. 1*C*). The neuronal cell death observed 3 h after NMDA exposure was not accompanied by significant caspase-3 activation (863 ± 39 pmol AMC/mg/min in control cells vs 601 ± 29 pmol AMC/mg/min in NMDA-treated cells; $n = 3$), indicating that acute neuronal cell death was attributable to necrosis but not apoptosis.

Sensitivity of excitotoxic varicosity formation and neuronal cell death to Cl^- channel blockers

Twenty minute exposure to NMDA induced the formation of varicosities in ~80% of the cultured cortical neurons (Fig. 2*A*). In the presence of NPPB (40 μM), phloretin (100 μM), or IAA-94 (1 mM), which are known blockers of the VSOR Cl^- channel in mouse cortical neurons (Inoue et al., 2005), varicosity formation was significantly, although not completely, inhibited (Fig. 2*A*). Because our preliminary patch-clamp study showed that the cultured neurons express a ligand-gated $GABA_A$ receptor Cl^- chan-

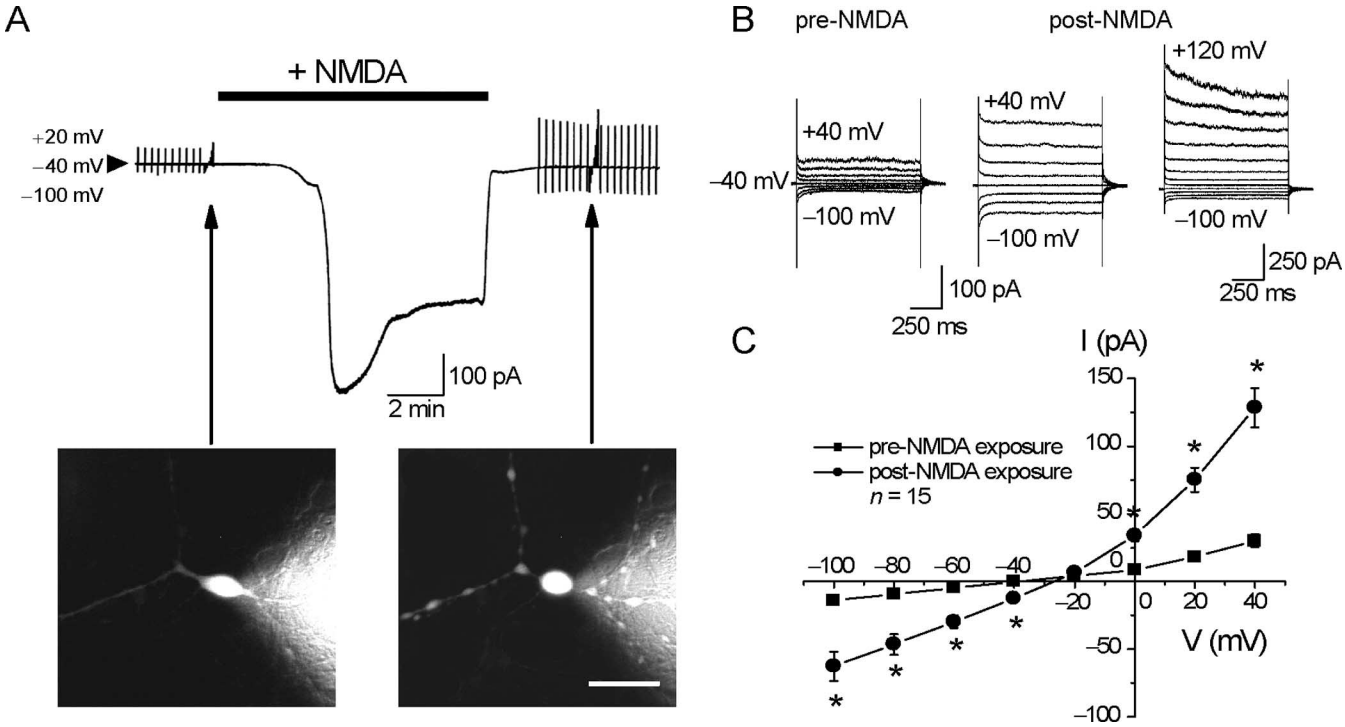

Figure 4. Whole-cell Cl^- currents activated after NMDA exposure in cultured mouse cortical neurons. ***A***, Representative trace showing Cl^- current activation after sublethal stimulation with NMDA (30 μM for 10 min). Alternating pulses (2 s duration, every 15 s) or step pulses from −100 to +40 mV in 20 mV increments (at arrows) were applied to elicit currents in the absence of NMDA; during NMDA exposure, the membrane potential was held at −40 mV. Arrowhead represents the zero-current level. Insets, Fluorescence micrographs captured before (left) and after (right) exposure to NMDA. Calcein (5 μM) was introduced via the pipette solution. Scale bar, 30 μm. ***B***, Expanded traces of current responses to step pulses from −100 to +40 mV (left and middle traces) or +120 mV (right traces) in 20 mV increments. Inactivation could be seen at large positive potentials (more than or equal to +80 mV). ***C***, Current–voltage relationships of Cl^- currents recorded before (squares) and after (circles) exposure to NMDA. *At given voltages, data points designated with circles that were significantly different from those designated with squares at $p < 0.05$. Each symbol represents the mean ± SEM (error bars).

nels (data not shown), the effects of their blockers on varicosity formation were next examined. $GABA_A$ receptor Cl^- channel blockers bicuculline (10 μM) and picrotoxin (100 μM) also inhibited varicosity formation significantly, although less prominently than a VSOR Cl^- channel blocker IAA-94 (Fig. 2*A*). An additive effect was observed when NPPB and picrotoxin were coadministered (Fig. 2*A*). However, bumetanide (10 μM) and furosemide (1 mM), which are blockers of the Na^+-K^+-2Cl^- cotransporter (NKCC) and K^+-Cl^- cotransporter (KCC), respectively, failed to suppress varicosity formation (Fig. 2*A*). These results suggest that varicosity formation results from the influx of Cl^- through multiple pathways including the VSOR Cl^- channel and $GABA_A$ receptor Cl^- channel but not the electroneutral cotransporters NKCC and KCC.

The level of neuronal necrosis was assessed 3 h after NMDA exposure by both LDH release (Figs. 1*C*, 2*B*) and PI staining (Fig. 2*C*). NMDA-induced necrosis was strongly inhibited by VSOR Cl^- channel blockers (NPPB, phloretin, and IAA-94). In contrast, neither $GABA_A$ Cl^- channel blockers (bicuculline and picrotoxin) nor chloride transporter blockers (bumetanide and furosemide) affected neuronal cell death (Fig. 2*B*,*C*). A glycine receptor channel blocker, strychnine (50 nM), did not suppress either varicosity formation or LDH release (data not shown).

These data suggest that the VSOR Cl^- channel serves as a major pathway for Cl^- influx, which is responsible for the persistence of dendritic beadings and neuronal swelling that lead to necrotic cell death in cultured cortical neurons.

Sensitivity of varicosity resolution after sublethal glutamate receptor stimulation to Cl^- channel blockers

Dendritic beadings induced by 10 min exposure to NMDA in cultured cortical neurons were not associated with a significant loss of membrane integrity, as judged by LDH release (Fig. 1*C*). The varicosities induced by such a brief and sublethal excitotoxic insult were found to be resolved in a time-dependent manner, as shown in Figure 3*A*. VSOR Cl^- channel blockers, NPPB (40 μM), phloretin (100 μM), and IAA-94 (1 mM), applied after washout of NMDA abolished the recovery from the varicosities (Fig. 3*B*). In contrast, neither the $GABA_A$ receptor Cl^- channel blockers bicuculline and picrotoxin, nor the NKCC and KCC blockers bumetanide and furosemide significantly affected recovery from the varicosities (Fig. 3*B*). Thus, it is suggested that VSOR Cl^- channels are functionally expressed on varicosities and are involved in recovery from varicosities after washout of NMDA.

Activation of whole-cell VSOR Cl^- channel current after sublethal glutamate-receptor stimulation

To confirm that the VSOR Cl^- channel is involved in the recovery from varicosities, whole-cell patch-clamp recordings were first performed in primary cultured cortical neurons. In the absence of NMDA, cortical neurons exhibited only small inward currents during exposure to Na^+-rich, low-Mg^{2+} HBS, and there was no obvious difference between the amplitudes of Cl^- currents recorded before and after exposure to Na^+-rich, low-Mg^{2+} HBS (data not shown). In contrast, during exposure of neurons to Na^+-rich, low-Mg^{2+} HBS containing 30 μM NMDA,

large inward currents were observed (Fig. 4*A*). Because the inward currents were inhibited by application of an NMDA receptor antagonist, 100 μM MK801 or 50 μM APV (supplemental Fig. 1, available at www.jneurosci.org as supplemental material), the currents were mainly mediated by NMDA receptor cation channels. After washing out of NMDA and returning the cells to NMDG-Cl solution, the basal current became significantly larger than it was before exposure to NMDA (Fig. 4*A*). When neurons were visualized with fluorescent calcein introduced into the cytosol via pipette solution during whole-cell recordings, it was found that this Cl^- current activation was accompanied by varicosity formation (Fig. 4*A*, insets). The activated currents exhibited outward rectification (Fig. 4*B*,*C*) and time-dependent inactivation at strong depolarizing potentials (Fig. 4*B*). The E_{rev} value was -25.9 ± 1.3 mV ($n = 15$) (Fig. 4*C*), which is much closer to E_{Cl} (−40.9 mV) than E_{Na} (−1.4 mV). This result suggests that the activated currents are selective not only to Cl^- but also to other anion species (aspartate$^-$ under the present conditions). Actually, separate whole-cell patch-clamp studies showed that the VSOR channel current activated by hypotonic stress (87.5% osmolarity) exhibits significant permeability to aspartate$^-$ ($P_{Asp}/P_{Cl} = 0.15 \pm 0.001$; $n = 8$). Thus, the E_{rev} value turns out to be close to the equilibrium potential to anions (−30.1 mV). As shown in Figure 5, the current increase after washout of NMDA was rapidly inhibited by the anion channel blockers NPPB (80 μM), phloretin (100 μM), and IAA-94 (1 mM). These electrophysiological and pharmacological properties of the increased basal current observed after washout of NMDA are essentially identical to those of the VSOR Cl^- channel current observed after osmotic swelling in cortical neurons (Inoue et al., 2005).

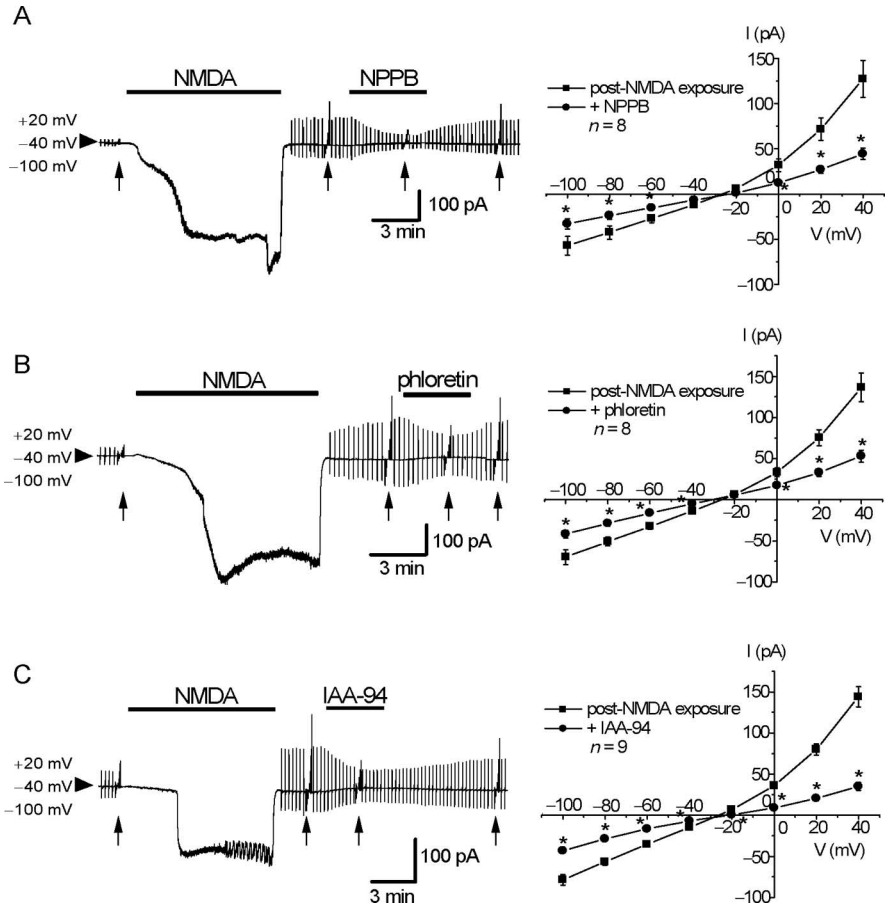

Figure 5. ***A–C***, Effects of 80 μM NPPB (***A***), 100 μM phloretin (***B***), and 1 mM IAA-94 (***C***) on Cl^- currents activated after NMDA exposure in cultured mouse cortical neurons. Left, Representative current records before, during, and after sublethal stimulation with NMDA (30 μM for 10 min) in the absence and presence of NPPB, phloretin, or IAA-94 added to the bathing solution. Alternating pulses (2 s duration, every 15 s) or step pulses from −100 to +40 mV in 20 mV increments (at arrows) were applied to record currents in the absence of NMDA; during NMDA exposure, the membrane potential was held at −40 mV. Arrowheads represent the zero-current level. Right, Current–voltage relationships in the absence (squares) and presence (circles) of NPPB, phloretin, or IAA-94. Each symbol represents the mean current ± SEM (error bars). *At given voltages, data points designated with circles that were significantly different from those designated with squares at $p < 0.05$.

Activation of whole-cell VSOR Cl^- channel current in association with excitotoxic neuronal swelling

Because varicosity formation was clearly observed after NMDA exposure during whole-cell recordings (Fig. 4*A*), we tested the possibility that the activation of the VSOR Cl^- channel in cultured cortical neurons is a consequence of neuronal swelling. Application of hypertonic solution (400 mOsm) inhibited the activated currents (Fig. 6*A*). Under Na^+-free conditions, Cl^- currents could not be activated by NMDA exposure (Fig. 6*B*). Exposure to Na^+-rich solution containing 1 μM AMPA and 2.5 μM cyclothiazide induced the activation of inward currents (Fig. 6*C*) as large as those activated by exposure to 30 μM NMDA. The AMPA exposure-induced Cl^- current exhibited the same properties as the NMDA exposure-induced Cl^- current: NPPB sensitivity and outward rectification (Fig. 6*C*), as well as inactivation kinetics at large positive potentials (data not shown). On balance, it is concluded that activation of the VSOR Cl^- channel in cultured neurons is induced by excitotoxic stimulation, presumably because of neuronal swelling resulting from Na^+ influx through either NMDA-type or AMPA-type glutamate receptor channels.

Activation of VSOR Cl^- channel single-channel events on dendritic varicosities formed by excitotoxicity stimulation

The existence of VSOR Cl^- channels on varicosities was then tested in cultured cortical neurons using the on-varicosity patch-clamp and the perforated-vesicle outside-out patch-clamp techniques. On-varicosity recordings revealed that VSOR Cl^- channels on varicosities were active during NMDA exposure (Fig. 7*A*). Time-dependent closing events could clearly be observed at large positive potentials ($-V_P > +80$ mV). The unitary slope conductance, which was ~75 pS at positive potentials (from +40 to +100 mV) and ~22 pS at negative potentials (from −120 to −80 mV), exhibited outward rectification. In the perforated-vesicle outside-out patch configuration made by withdrawing the pipette from the varicosity, similar single-channel events could also be observed (Fig. 7*B*). Time-dependent closing events could consistently be observed at +140 mV. Extracellular application of NPPB (80 μM) initially induced flickery block of single-channel currents in a reversible manner (Fig. 7*B*). The single-channel currents were then completely abolished after application of

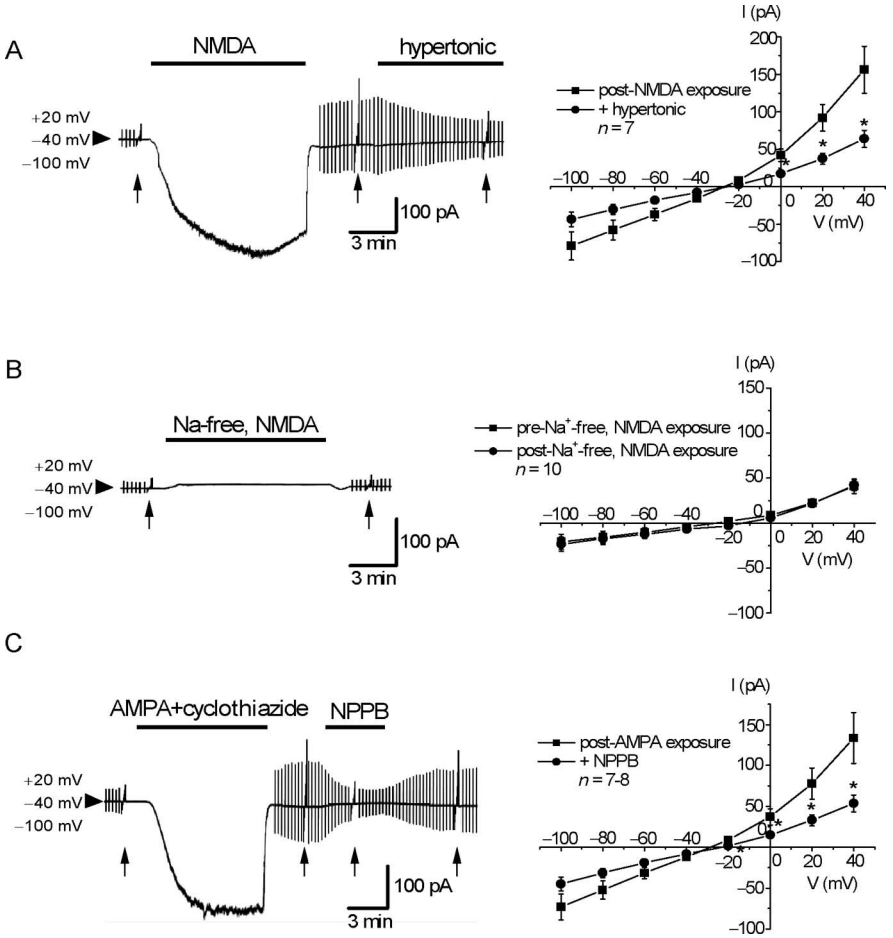

Figure 6. Dependence of Cl^- currents activated after glutamate receptor stimulation on swelling and Na^+ influx in cultured mouse cortical neurons. ***A***, Effects of osmotic shrinkage induced by hypertonic solution (400 mOsm) on Cl^- currents activated after sublethal stimulation with NMDA (30 μM for 10 min). ***B***, Effects of Na^+ removal during NMDA exposure on activation of Cl^- currents after NMDA exposure. ***C***, Effects of stimulation with AMPA (1 μM) plus cyclothiazide (2.5 μM) for 10 min on activation of Cl^- currents. Left, Representative records of currents before, during, and after stimulation with NMDA or AMPA, and sensitivity to NPPB and hypertonicity. Alternating pulses (2 s duration, every 15 s) or step pulses from −100 to +40 mV in 20 mV increments (at arrows) were applied to record currents in the absence of NMDA or AMPA; during exposure to NMDA or AMPA, the membrane potential was held at −40 mV. Arrowheads represent the zero-current level. Right, Current–voltage relationships of NMDA-activated currents recorded under isotonic (squares) and hypertonic (circles) conditions (***A***), of currents recorded before (squares) and after (circles) exposure to Na^+-free, low-Mg^{2+} solution containing 30 μM NMDA (***B***), or of AMPA-activated currents in the absence (squares) and presence (circles) of 80 μM NPPB (***C***). Each symbol represents the mean current ± SEM (error bars). *At given voltages, data points designated with circles that were significantly different from those designated with squares at $p < 0.05$.

NPPB for ≥10 min (data not shown). The unitary slope conductance, which was ~56 pS at positive potentials (from +100 to +160 mV) and ~13 pS at negative potentials (from −100 to −60 mV), exhibited outward rectification. These data demonstrate that NMDA-induced varicosities do in fact express active VSOR Cl^- channels in cultured cortical neurons during exposure to NMDA.

VSOR Cl^- channels are expressed in brain slices, in which they are involved in excitotoxic neuronal cell death

To examine whether the VSOR Cl^- channel functions in more physiological situations, we next examined, using a slice-patch technique, the functional expression of VSOR Cl^- channels in layer V pyramidal neurons in barrel cortex slices of young adult mice. Under the whole-cell configuration, the application of hypotonic solution (81.7% osmolarity) gradually activated whole-cell currents (Fig. 8*A*). This current exhibited outward rectification and inactivation kinetics at large positive potentials (Fig. 8*B*, middle). The activated currents were inhibited by either IAA-94 (1 mM) or hypertonic solution (400 mOsm/kg-H_2O) (Fig. 8*B-D*). When ATP was absent from in the intracellular pipette solution, the current activation was largely attenuated (Fig. 8*D*). This observation is in good agreement with the known cytosolic ATP dependence of VSOR Cl^- channel activation (Okada, 1997). When the extracellular Cl^- concentration was decreased from 110.5 to 30.5 mM, the reversal potential was shifted to a more positive potential (from −41.9 ± 1.3 to −34.6 ± 1.2 mV; $n = 7$). These results indicate that the layer V neurons in the slice preparation express the VSOR Cl^- channel.

To examine the involvement of the VSOR Cl^- channel in excitotoxic cell death in brain slices, cell death was monitored by PI uptake in brain slices after they were incubated in ACSF containing 30 μM NMDA in the presence or absence of a Cl^- channel blocker (Fig. 9, for higher magnification colored photographs, see supplemental Fig. 2, available at www.jneurosci.org as supplemental material). When the brain slices were incubated in control ACSF for 1 h, PI signals were observed only in the surface region of the slice (Fig. 9*A*, control). These PI signals are likely to result from cell death caused by the cutting during the slice preparation. In contrast, the brain slice exposed to NMDA-containing ACSF showed massive staining with PI not only in the surface region, but also in the deep regions of the slices (Fig. 9*A*, NMDA). In the presence of 1 mM IAA-94, NMDA-induced cell death was significantly reduced (Fig. 9*A*, +IAA-94). Consistent with the results obtained in cultured cortical neurons, 10 μM bicuculline failed to inhibit NMDA-induced cell death (Fig. 9*B*). Thus, it is concluded that in cortical neurons in brain slices, the VSOR Cl^- channel, but not the $GABA_A$ Cl^- channel, plays an important role in the progression of excitotoxic cell death.

Discussion

Cell volume regulation is an essential function in all animal cells, because persistent shrinkage or swelling is associated with apoptotic and necrotic cell death (Okada et al., 2001, 2004). In neurons, even a temporary volume increase is known to induce alterations in excitability such as enhanced epileptiform bursting (Dudek et al., 1990; Azouz et al., 1997) and spreading depression (Chebabo et al., 1995). Excitotoxic insults induce prominent swelling of the neuronal soma and dendrites in a manner dependent on extracellular Cl^- (Rothman, 1985; Olney et al., 1986; Choi, 1987; Dessi et al., 1994; Hasbani et al., 1998; Inglefield and Schwartz-Bloom, 1998; Sakaguchi et al., 1999). Under excito-

toxic conditions, volume regulation was inhibited in cortical neurons (Churchwell et al., 1996). Thus, it is important to investigate the activity and roles of volume-regulatory Cl^- channels in cortical neurons during and after an excitotoxic insult.

Activation of the neuronal VSOR Cl^- channel is induced by excitotoxic stimulation

Our previous study (Inoue et al., 2005) demonstrated that the VSOR Cl^- channel is robustly expressed on both the soma and dendrites in mouse cortical neurons and is activated by hypotonicity-induced osmotic swelling. Likewise, the present study demonstrated that pyramidal neurons in brain slices acutely prepared from mouse somatosensory barrel cortex express the VSOR Cl^- channel (Fig. 8). Using both whole-cell and single-channel patch-clamp techniques in the present study, we show that the VSOR Cl^- channel in mouse cortical neurons is activated by excitotoxic stimulation with not only NMDA, but also AMPA (Figs. 4–7). It appears that neuronal swelling induced by activation of the glutamate receptor-linked cation channel is responsible for activation of the VSOR Cl^- channel, because channel activation was inhibited when osmotic swelling was suppressed by application of hypertonic solution (Fig. 6*A*) or by abolition of Na^+ inflow under Na^+-free conditions (Fig. 6*B*). The fact that the VSOR Cl^- channel was found to be active during (Fig. 7) and after (Figs. 4–6) excitotoxic stimulation suggests that the channel plays volume-related roles during both stages (see below).

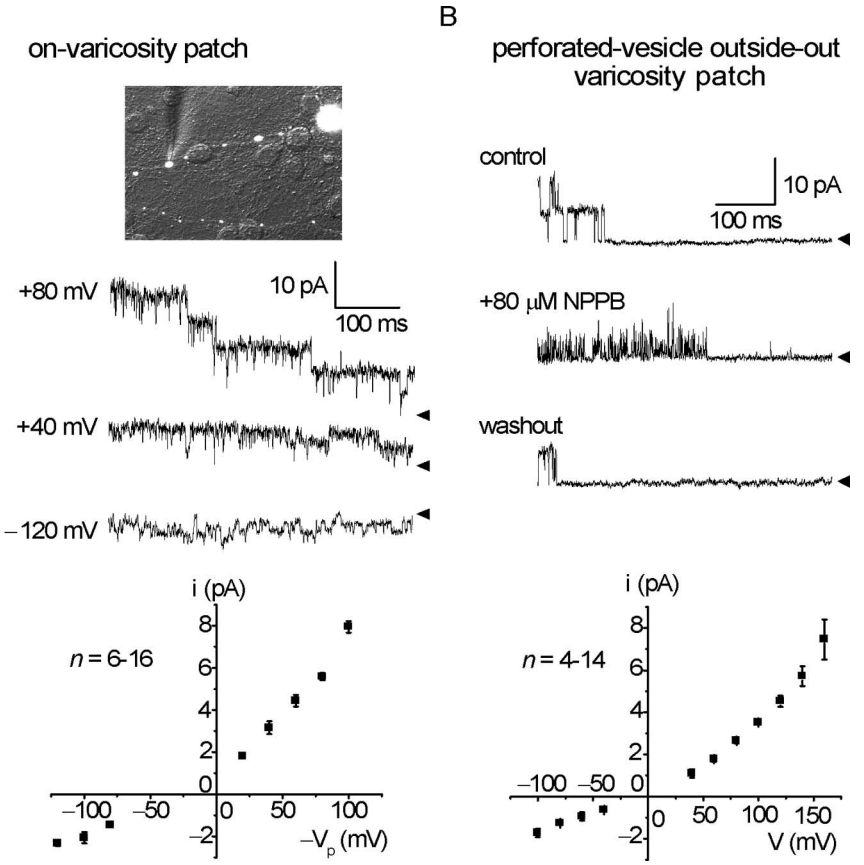

Figure 7. Single-channel recordings from varicosities induced by NMDA exposure in cultured mouse cortical neurons. ***A***, Unitary current records from on-varicosity patches. Top, Micrograph of the on-cell configuration formed on a varicosity in an EGFP-expressing neuron after NMDA exposure. Middle, Representative traces of single-channel currents recorded from a varicosity during NMDA exposure. Varying step pulses ($-V_p$) were applied from a holding potential of −40 mV at the onset of the traces. Arrowheads represent the zero-current level. Bottom, Current–voltage relationship for single-channel events recorded from on-varicosity patches. ***B***, Unitary current records from perforated-vesicle outside-out patches excised from varicosities. After perforation (monitored by series resistance), the pipette was lifted up to make the perforated-vesicle patch configuration. Top, Representative traces of single-channel currents at their onset, elicited with application of a voltage step from a holding potential of 0 to +140 mV. An 80 μM concentration of NPPB reversibly inhibited single-channel currents. Arrowheads represent the zero-current level. Bottom, Current–voltage relationship for single-channel events recorded from perforated-vesicle outside-out varicosity patches. Each symbol represents the mean unitary current (i) ± SEM (error bars).

Neuronal VSOR Cl^- channels activated after sublethal excitotoxic stimulation are involved in varicosity resolution

Consistent with previous observations (Park et al., 1996; Faddis et al., 1997; Hasbani et al., 1998, 2001; Zhang et al., 2005), cerebral cortical neurons could recover from somatic swelling (Fig. 1*A*) and resolve varicosities (Fig. 3*A*) within 60 min after sublethal excitotoxic stimulation. Because the VSOR Cl^- channel was activated during this period (Figs. 4–6), it was expected that the channel would play a volume-regulatory role by releasing anionic osmolytes from the cells and thereby driving the efflux of osmotically obliged water after washout of excitotoxins. Indeed, application of VSOR Cl^- channel blockers was found to completely prevent varicosity resolution (Fig. 3*B*). In contrast, blockers of the $GABA_A$ receptor Cl^- channel, NKCC and KCC, failed to inhibit recovery from dendritic swelling after termination of excitotoxic stimulation (Fig. 3*B*). Thus, it is concluded that, in cultured cortical neurons, VSOR Cl^- channels, but not $GABA_A$ receptors or Cl^- transporters, serve as the pathway for volume-regulatory anion efflux and play a requisite role in varicosity resolution after a sublethal excitotoxic insult.

Neuronal VSOR Cl^- channels activated during excitotoxic stimulation are involved in varicosity formation

Although it was found that some volume-regulatory pathway is disrupted during activation of NMDA receptors in cortical neurons (Churchwell et al., 1996), we were able to consistently observe robust activity of the VSOR Cl^- channel, which plays a volume-regulatory role in nonexcitotoxic swollen neurons (Inoue et al., 2005), on varicosities during NMDA receptor stimulation (Fig. 7). It must be noted, however, that dendritic and somatic swelling induced by stimulation with NMDA (Fig. 1) were coupled to profound depolarization in mouse cortical neurons, as observed in brain slices by an optical recording method (Sato et al., 1997). Under such marked depolarizing conditions, the VSOR Cl^- channel would be unable to serve as the pathway for volume-regulatory Cl^- efflux, but rather might serve as the pathway for swelling-aggravating Cl^- influx. Indeed, coapplication of VSOR Cl^- channel blockers with NMDA alleviated neuronal varicosity formation (Fig. 2*A*). Because $GABA_A$ receptor blockers were also effective in suppressing varicosity formation (Fig. 2*A*), it seems likely that swelling-inducing Cl^- influx initially takes

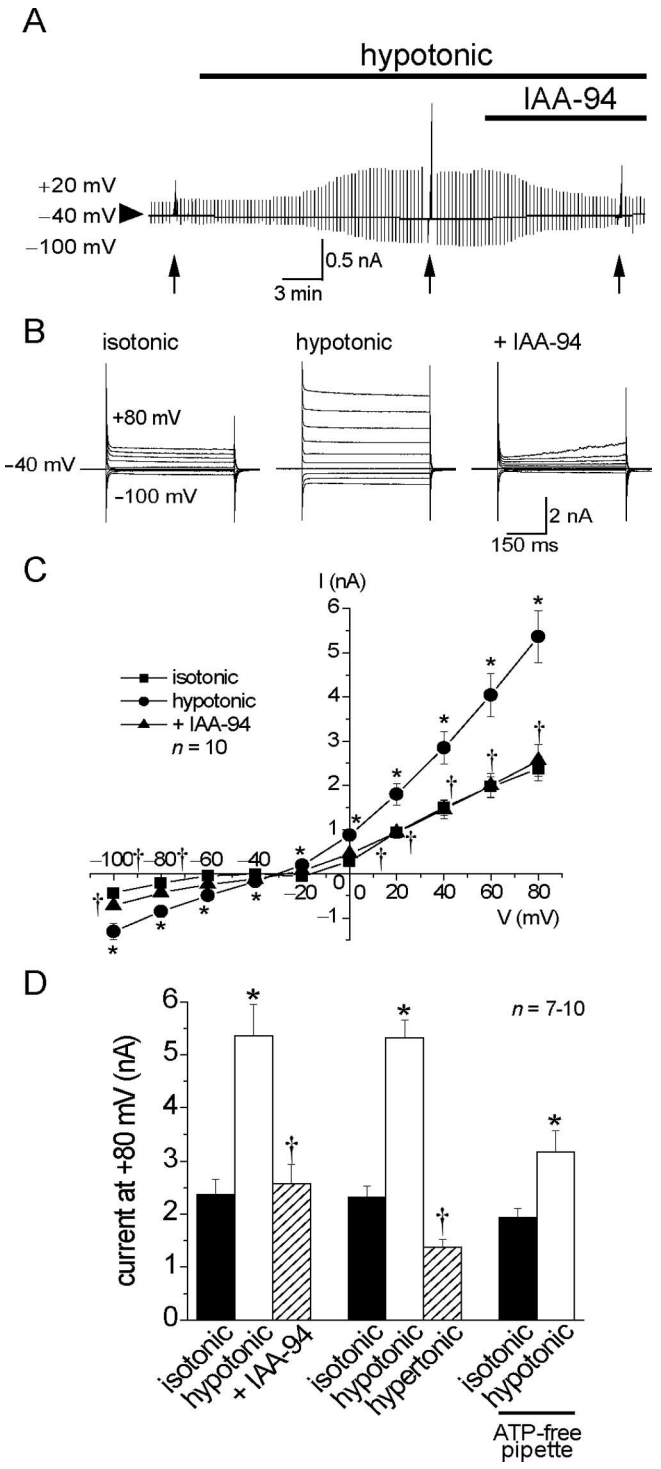

Figure 8. Whole-cell Cl^- currents activated by hypotonic stress in mouse layer V neurons in slices of the barrel cortex. ***A***, Representative trace showing current activation after hypotonic stress. Alternating pulses (2 s duration, every 15 s) or step pulses from −100 to +80 mV in 20 mV increments (at arrows) were applied to elicit currents. ***B***, Expanded traces of current responses to step pulses (arrows in ***A***) under isotonic (left) or hypotonic conditions in the absence (middle) or presence (right) of IAA-94 (1 mM). Inactivation kinetics could be seen at +80 mV in currents activated by hypotonic stress in the absence of IAA-94. ***C***, Current–voltage relationships under the isotonic (squares) or hypotonic conditions in the absence (circles) or presence (triangles) of IAA-94. ***D***, The effects of IAA-94 (1 mM), hypertonicity (400 mOsm) or intracellular ATP removal on current activation induced by hypotonic stress at +80 mV. $*p < 0.05$ versus isotonic. $^{\dagger}p < 0.05$ versus hypotonic. Each symbol or column represents the mean ± SEM (error bars).

place mainly via $GABA_A$ receptor Cl^- channel and that additional Cl^- influx is carried by VSOR Cl^- channels activated later by swelling. Whatever the time course of activation, it is clear that both $GABA_A$ receptors and VSOR Cl^- channels are involved in excitotoxic varicosity formation. This conclusion is in good agreement with a previous suggestion that multiple Cl^- influx pathways are involved in varicosity formation in mouse cortical neurons (Hasbani et al., 1998).

Neuronal VSOR Cl^- channels activated during excitotoxic stimulation are involved in necrotic neuronal cell death

Prolonged stimulation of ionotropic glutamate receptors results in excitotoxic neuronal death. In the present study, exposure to NMDA was found to induce prominent death both of cultured cortical neurons of mouse embryos (Fig. 2*B*,*C*) and of cortical neurons in brain slices of young adult mice (Fig. 9). Because both LDH release and PI uptake are markers of breakdown of the plasma membrane, neuronal cell death induced by such acute excitotoxicity may represent necrosis but not apoptosis. Indeed, significant activation of caspase-3 was never observed in cultured neurons 3 h after NMDA exposure in this study.

Although NMDA-induced varicosity formation was sensitive to both VSOR Cl^- channel blockers and $GABA_A$ receptor blockers (Fig. 2*A*), NMDA-induced necrosis of mouse embryonic cortical neurons in culture (Fig. 2*B*,*C*) and young adult cortical neurons in slices (Fig. 9) was sensitive solely to VSOR Cl^- channel blockers. Thus, it appears that persistent Cl^- influx, which is followed by necrosis is the results of prolonged activation of the VSOR Cl^- channel, but not of the $GABA_A$ receptor in both embryonic and young adult cortical neurons. In fact, coapplication of $GABA_A$ receptor agonist GABA or muscimol failed to enhance NMDA-induced necrosis of cultured cortical neurons (H. Inoue, unpublished observations). In spinal motor neurons (Van Damme et al., 2003) and cerebellar granule cells (Babot et al., 2005), excitotoxic Cl^- influx which is associated with neuronal cell death was shown to be mediated by some anion channels that are distinct from the $GABA_A$ receptor and sensitive to NPPB and niflumate. In mouse cortical neurons, the VSOR Cl^- channel, which was activated on NMDA-induced varicosities was also sensitive to NPPB (Fig. 7) and niflumate (H. Inoue, unpublished observations). It is therefore possible that the VSOR Cl^- channel is also responsible for the Cl^- influx involved in excitotoxic death in spinal motor neurons and cerebellar granule cells.

In brain, swelling-induced glutamate release is largely mediated by VSOR Cl^- channels (Kimelberg, 2004, 2005; Liu et al., 2006), which are permeable to glutamate (Strange et al., 1996; Okada, 1997). If this is the case for excitotoxic neuronal swelling, glutamate released via NMDA-activated VSOR Cl^- channels may activate additional glutamate receptors including both NMDA and AMPA receptors. The VSOR Cl^- channel may thus promote influx of not only Cl^-, but also Na^+, thereby aggravating NVI and excitotoxic neuronal injury.

Synopsis and conclusions: dual roles of VSOR Cl^- channel in excitotoxic neuronal responses

On balance, the VSOR Cl^- channel plays dual, reciprocal roles in excitotoxic neurons, as schematically depicted in Figure 10. Excitotoxic neuronal swelling is expected to occur by water inflow driven by Na^+ influx via glutamate receptor (GluR) cation channels and Cl^- influx via $GABA_A$ receptor ($GABA_AR$) anion channels; that is because NMDA stimulation was reported to cause GABA release in primary cultures (Erdö et al., 1993), which are known to contain GABAergic neurons (Dichter, 1980). Somatic

and dendritic swelling then activates the VSOR Cl^- channel (process 1). Under marked depolarization induced by GluR, the VSOR Cl^- channel would serve as a pathway for swelling-aggravating Cl^- influx (process 1 to 2). This Cl^- inflow-mediating activity of VSOR Cl^- channel may explain why volume regulation is impaired in cortical neurons under excitotoxic conditions (Churchwell et al., 1996). However, when neurons repolarize after washout of NMDA, VSOR Cl^- channel activity may be responsible for the volume-regulatory Cl^- efflux (process 4). In this recovery process, volume-regulatory K^+ efflux may be mediated by some K^+ channel, because K^+ channel blockers Ba^{2+} and quinine were found to block varicosity resolution after washout of NMDA (H. Inoue, unpublished observations). However, prolonged excitotoxic insults result in persistent depolarization and thereby lead to persistent swelling in the soma and dendrites not only because of continuing inflow of Na^+, Cl^-, and osmotically obliged water, but also because of impaired mechanisms of volume regulation. Thus, VSOR Cl^- channel activation plays a key role in NVI (process 2 to 3). In this study, both varicosity resolution attained after sublethal excitotoxic stimulation and NMDA-induced necrosis of cortical neurons were found to be inhibited by VSOR Cl^- channel blockers but not by blockers of $GABA_AR$, NKCC, or KCC. Thus, it is clear that the VSOR Cl^- channel serves as a Cl^- flux pathway essential for either recovery from or persistence of excitotoxic neuronal injury, depending on the membrane potential level.

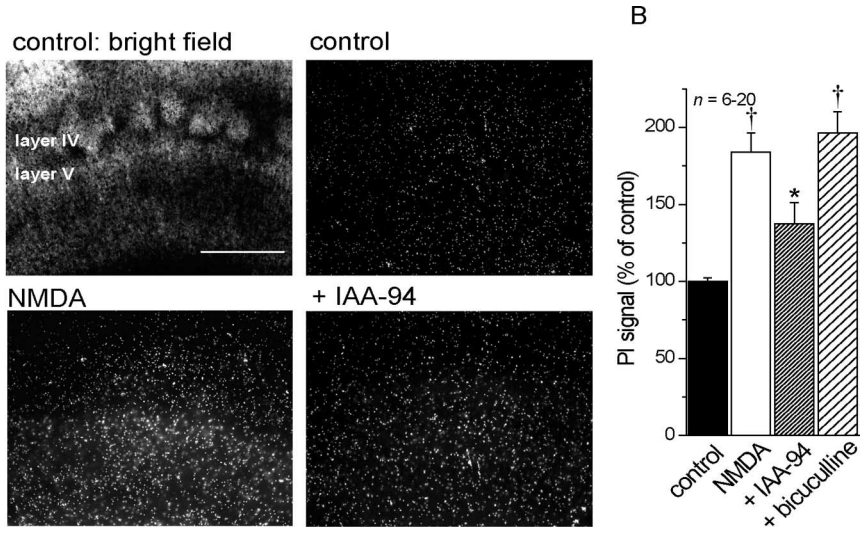

Figure 9. Necrotic cell death induced by NMDA receptor activation and its sensitivity to Cl^- channel blockers in brain slices. ***A***, Representative PI staining of slices taken 1 h after incubation in control or NMDA-containing ACSF with or without IAA-94 (1 mM). A representative bright-field image of a brain slice used in the present study is shown in the top left (control). Clear column structures can be seen in layer IV. PI signal increased in the slice treated with 30 μM NMDA. Application of IAA-94 decreased NMDA-induced cell death. Scale bar, 500 μm. ***B***, Normalized PI signals in the brain slices. NMDA (30 μM) increased neuronal injury. IAA-94 (1 mM) but not bicuculline (10 μM) reduced cell injury induced by application of 30 μM NMDA. $^*p < 0.05$ versus NMDA. $^\dagger p < 0.05$ versus control. Each column represents the mean ± SEM (error bars).

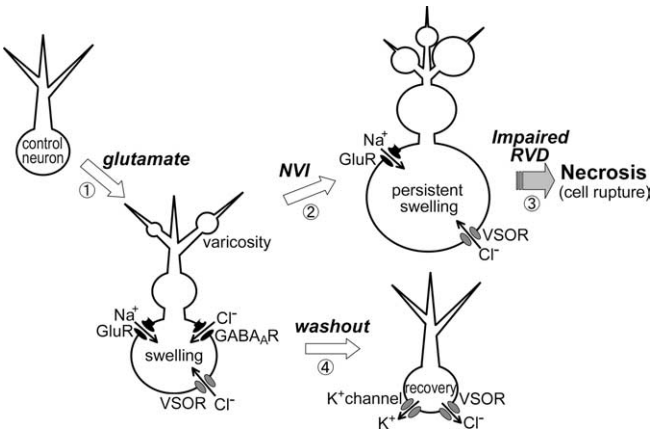

Figure 10. Schematic illustration of dual roles of the VSOR Cl^- channel in mouse cortical neurons under excitotoxic conditions. The VSOR Cl^- channel is activated during excitotoxic glutamate stimulation and leads to formation of varicosities (process 1), and later to NVI (process 2) and necrotic cell death (process 3), by inducing NaCl influx in cooperation with GluR cation channels in both process 1 and 2, as well as with $GABA_AR$ anion channels in process 1. The VSOR Cl^- channel is also activated after washout of glutamate and leads to resolution of varicosities (process 4) by inducing KCl efflux in cooperation presumably with K^+ channels. GluR-mediated Ca^{2+} influx, which is known to be another key element of glutamate toxicity, is not included in this scheme.

References

Azouz R, Alroy G, Yaari Y (1997) Modulation of endogenous firing patterns by osmolarity in rat hippocampal neurones. J Physiol (Lond) 502:175–187.

Babot Z, Cristófol R, Suñol C (2005) Excitotoxic death induced by released glutamate in depolarized primary cultures of mouse cerebellar granule cells is dependent on $GABA_A$ receptors and niflumic acid-sensitive chloride channels. Eur J Neurosci 21:103–112.

Barros LF, Hermosilla T, Castro J (2001) Necrotic volume increase and the early physiology of necrosis. Comp Biochem Physiol A Mol Integr Physiol 130:401–409.

Chebabo SR, Hester MA, Aitken PG, Somjen GG (1995) Hypotonic exposure enhances synaptic transmission and triggers spreading depression in rat hippocampal tissue slices. Brain Res 695:203–216.

Chen Q, Moulder K, Tenkova T, Hardy K, Olney JW, Romano C (1999) Excitotoxic cell death dependent on inhibitory receptor activation. Exp Neurol 160:215–225.

Choi DW (1987) Ionic dependence of glutamate neurotoxicity. J Neurosci 7:369–379.

Churchwell KB, Wright SH, Emma F, Rosenberg PA, Strange K (1996) NMDA receptor activation inhibits neuronal volume regulation after swelling induced by veratridine-stimulated Na^+ influx in rat cortical cultures. J Neurosci 16:7447–7457.

Dessi F, Charriaut-Marlangue C, Ben Ari Y (1994) Glutamate-induced neuronal death in cerebellar culture is mediated by two distinct components: a sodium-chloride component and a calcium component. Brain Res 650:49–55.

Dichter MA (1980) Physiological identification of GABA as the inhibitory transmitter for mammalian cortical neurons in cell culture. Brain Res 190:111–121.

Dudek FE, Obenaus A, Tasker JG (1990) Osmolality-induced changes in extracellular volume alter epileptiform bursts independent of chemical synapses in the rat: importance of non-synaptic mechanisms in hippocampal epileptogenesis. Neurosci Lett 120:267–270.

Erdö SL, Cai N, Lakics V (1993) Medium-dependent dissociation of cytotoxic and GABA-releasing effects of N-methyl-D-aspartate (NMDA), alpha-amino-3-hydroxy-5-methyl-4-isoxazolepropionate (AMPA) and kainate in rat cortical cultures. Neurosci Lett 152:84–86.

Faddis BT, Hasbani MJ, Goldberg MP (1997) Calpain activation contributes to dendritic remodeling after brief excitotoxic injury *in vitro*. J Neurosci 17:951–959.

Goel S, Wharton SB, Brett LP, Whittle IR (2003) Morphological changes and stress responses in neurons in cerebral cortex infiltrated by diffuse astrocytoma. Neuropathology 23:262–270.

Goldberg MP, Choi DW (1993) Combined oxygen and glucose deprivation in cortical cell culture: calcium-dependent and calcium-independent mechanisms of neuronal injury. J Neurosci 13:3510–3524.

Hasbani MJ, Hyrc KL, Faddis BT, Romano C, Goldberg MP (1998) Distinct roles for sodium, chloride, and calcium in excitotoxic dendritic injury and recovery. Exp Neurol 154:241–258.

Hasbani MJ, Schlief ML, Fisher DA, Goldberg MP (2001) Dendritic spines lost during glutamate receptor activation reemerge at original sites of synaptic contact. J Neurosci 21:2393–2403.

Hogan RN, Baringer JR, Prusiner SB (1987) Scrapie infection diminishes spines and increases varicosities of dendrites in hamsters: a quantitative Golgi analysis. J Neuropathol Exp Neurol 46:461–473.

Hori N, Carpenter DO (1994) Functional and morphological changes induced by transient in vivo ischemia. Exp Neurol 129:279–289.

Hsu M, Buzsáki G (1993) Vulnerability of mossy fiber targets in the rat hippocampus to forebrain ischemia. J Neurosci 13:3964–3979.

Ikegaya Y, Kim JA, Baba M, Iwatsubo T, Nishiyama N, Matsuki N (2001) Rapid and reversible changes in dendrite morphology and synaptic efficacy following NMDA receptor activation: implication for a cellular defense against excitotoxicity. J Cell Sci 114:4083–4093.

Inglefield JR, Schwartz-Bloom RD (1998) Activation of excitatory amino acid receptors in the rat hippocampal slice increases intracellular Cl^- and cell volume. J Neurochem 71:1396–1404.

Inoue H, Mori S, Morishima S, Okada Y (2005) Volume-sensitive chloride channels in mouse cortical neurons: characterization and role in volume regulation. Eur J Neurosci 21:1648–1658.

Isokawa M, Levesque MF (1991) Increased NMDA responses and dendritic degeneration in human epileptic hippocampal neurons in slices. Neurosci Lett 132:212–216.

Johnson JW, Ascher P (1987) Glycine potentiates the NMDA response in cultured mouse brain neurons. Nature 325:529–531.

Kimelberg HK (2004) Water homeostasis in the brain: basic concepts. Neuroscience 29:851–860.

Kimelberg HK (2005) Astrocytic swelling in cerebral ischemia as a possible cause of injury and target for therapy. Glia 50:389–397.

Levitan ES, Kramer RH (1990) Neuropeptide modulation of single calcium and potassium channels detected with a new patch clamp configuration. Nature 348:545–547.

Liu H, Tashmukhamedov BA, Inoue H, Okada Y, Sabirov RZ (2006) Roles of two types of anion channels in glutamate release from mouse astrocytes under ischemic or osmotic stress. Glia 54:343–357.

Maeno E, Ishizaki Y, Kanaseki T, Hazama A, Okada Y (2000) Normotonic cell shrinkage because of disordered volume regulation is an early prerequisite to apoptosis. Proc Natl Acad Sci USA 97:9487–9492.

Matesic DF, Lin RC (1994) Microtubule-associated protein 2 as an early indicator of ischemia-induced neurodegeneration in the gerbil forebrain. J Neurochem 63:1012–1020.

Multani P, Myers RH, Blume HW, Schomer DL, Sotrel A (1994) Neocortical dendritic pathology in human partial epilepsy: a quantitative Golgi study. Epilepsia 35:728–736.

Nicklas WJ, Zeevalk G, Hyndman A (1987) Interactions between neurons and glia in glutamate/glutamine compartmentation. Biochem Soc Trans 15:208–210.

Okada Y (1997) Volume expansion-sensing outward rectifier Cl channel: A fresh start to the molecular identity and volume sensor. Am J Physiol 273:C755–C789.

Okada Y, Maeno E, Shimizu T, Dezaki K, Wang J, Morishima S (2001) Receptor-mediated control of regulatory volume decrease (RVD) and apoptotic volume decrease (AVD). J Physiol (Lond) 532:3–16.

Okada Y, Maeno E, Shimizu T, K Manabe, Mori S, Nabekura T (2004) Dual roles of plasmalemmal chloride channels in induction of cell death. Pflugers Arch 448:287–295.

Olney JW (1969) Brain lesion, obesity, and other disturbances in mice treated with monosodium glutamate. Science 164:719–721.

Olney JW, Price MT, Samson L, Labruyere J (1986) The role of specific ions in glutamate neurotoxicity. Neurosci Lett 65:65–71.

Park JS, Bateman MC, Goldberg MP (1996) Rapid alterations in dendrite morphology during sublethal hypoxia or glutamate receptor activation. Neurobiol Dis 3:215–227.

Reid SA, Sypert GW, Boggs WM, Willmore LJ (1979) Histopathology of the ferric-induced chronic epileptic focus in cat: a Golgi study. Exp Neurol 66:205–219.

Rothman SM (1985) The neurotoxicity of excitatory amino acids is produced by passive chloride influx. J Neurosci 5:1483–1489.

Sakaguchi T, Kuno M, Kawasaki K (1999) Disparity of cell swelling and rapid neuronal death by excitotoxic insults in rat hippocampal slice cultures. Neurosci Lett 274:135–138.

Sato K, Momose-Sato Y, Arai Y, Hirota A, Kamino K (1997) Optical illustration of glutamate-induced cell swelling coupled with membrane depolarization in embryonic brain stem slices. NeuroReport 8:3559–3563.

Scheibel ME, Crandall PH, Scheibel AB (1974) The hippocampal-dentate complex in temporal lobe epilepsy. A Golgi study. Epilepsia 15:55–80.

Sotrel A, Williams RS, Kaufmann WE, Myers RH (1993) Evidence for neuronal degeneration and dendritic plasticity in cortical pyramidal neurons of Huntington's disease: a quantitative Golgi study. Neurology 43:2088–2096.

Strange K, Emma F, Jackson PS (1996) Cellular and molecular physiology of volume-sensitive anion channels. Am J Physiol 270:C711–C730.

Van Damme P, Callewaert G, Eggermont J, Robberecht W, Van Den BL (2003) Chloride influx aggravates Ca^{2+}-dependent AMPA receptor-mediated motoneuron death. J Neurosci 23:4942–4950.

Watanabe SY, Albsoul-Younes AM, Kawano T, Itoh H, Kaziro Y, Nakajima S, Nakajima Y (1999) Calcium phosphate-mediated transfection of primary cultured brain neurons using GFP expression as a marker: application for single neuron electrophysiology. Neurosci Res 33:71–78.

Westrum LE, White Jr LE, Ward Jr AA (1964) Morphology of the experimental epileptic focus. J Neurosurg 21:1033–1046.

Yamada KA, Tang CM (1993) Benzothiadiazides inhibit rapid glutamate receptor desensitization and enhance glutamatergic synaptic currents. J Neurosci 13:3904–3915.

Zhang S, Boyd J, Delaney K, Murphy TH (2005) Rapid reversible changes in dendritic spine structure *in vivo* gated by the degree of ischemia. J Neurosci 25:5333–5338.